confluent 293 T cells in a T175 flask containing Opti-MEM medium and then incubated for 3 h. Next, these cells were cultured in DMEM containing 10% FBS. Virus-containing supernatants were harvested 4 days post transduction and concentrated by centrifugation (9,000 rpm, 6–8 h, 4°C). The virus pellet was resuspended in 1 ml of IMDM and used for overnight transduction of UT-7/EPO cells.

Transduction of the Lentiviral Library into UT-7/EPO Cells

UT-7/EPO cells were transduced with the viral cDNA library and cultured in methylcellulose semi-solid medium containing IMDM, 10% FBS, and P/S without EPO for one month. After this period, several colonies were harvested, and genomic DNA was isolated from each colony using the QIAamp DNA Micro Kit (Qiagen, Valencia, CA).

Genomic PCR and Sequence Analysis

The integrated cDNAs were PCR amplified using a forward primer (5′-TTCAGGTGTCGTGAACACGCTACCG-3′) and reverse primer (5′-CCTCGATGTTAACTCTAGAG GATCC-3′). The Expand Long Template PCR System (Roche, Basel, Switzerland) was used following the manufacturer's protocol. cDNAs that were cloned into the CSII-CMV-RfA vector were sequenced with the forward (5′-CAAGCCTCAGACAGTGG-3′) and reverse (5′-AGCG TATCCACATAGCG-3′) primers using a Big-Dye Terminator v3.1 Cycle sequencing kit (Applied Biosystems, Foster City, CA) and an ABI PRISM 3100 Genetic Analyzer (Applied Biosystems). The sequences were compared with the DNA database from the DNA Data Bank of Japan using BLAST.

Cell Culture and Sorting

The EPO-dependent UT-7/EPO cell line was established and cultured as previously reported [13]. C57BL6J mice and ICR mice were purchased from Nihon SLC. Twelve o'clock noon was considered to be 0.5 day postcoitum (dpc) for plugged mice. Fetal liver (FL) cells from a 12.5 dpc embryo were filtered through a 40 μM nylon mesh and washed with PBS. The cells were stained with a FITC-conjugated anti-mouse CD71 Ab (BD Biosciences), PE-conjugated anti-mouse Sca-1 Ab (BD Biosciences), APC-conjugated anti-mouse c-Kit Ab (BD Biosciences), PE-Cy7-conjugated anti-mouse CD45 Ab (eBioscience) and APC-Cy7-conjugated anti-mouse Ter119 Ab (eBioscience). The cells were sorted using a FACS Aria cell sorter (BDIS), and the data files were analyzed using FlowJo software (Tree Star, Inc.).

Human peripheral blood (PB) was obtained from healthy volunteers. The PB was stained with a FITC-conjugated anti-human CD45 Ab (eBioscience), PE-conjugated anti-GPA antibody (eBioscience) and APC-conjugated anti-human CD41 antibody (BD Bioscience). The cells were sorted using a FACS Aria cell sorter (BDIS), and the data files were analyzed using FlowJo software (Tree Star, Inc.).

All animal studies were approved by the Committee on Ethics in Animal Experiments of Kyushu University, and the human studies were approved by the Committee on Ethics in Human clinical samples of Kyushu University. All of these studies were performed following the guidelines of Kyushu University.

RNA Extraction and Real-time RT-PCR

Total RNA was isolated from FL cells of ICR embryos at 12.5 dpc or whole embryos at 10.5 dpc using the RNAqueous-4PCR kit (Ambion). Total RNA from human peripheral blood was isolated with the RiboPure Kit (Ambion). A high-capacity cDNA Archive kit (Applied Biosystems) was used to synthesize cDNA from RNA. The mRNA levels of various genes were analyzed by qRT-PCR using SYBR Green and gene-specific primers with the StepOnePlus real-time PCR system (Applied Biosystems). The mRNA level of each target gene was normalized to β-actin as an internal control.

Immunohistochemistry

Ter119-positive cells from 12.5 dpc FL cells were isolated by flow cytometry as described above. Cells were cytospun onto glass slides and air-dried. The cells were fixed in 1% PFA at room temperature (RT) for 10 min. Nonspecific binding was blocked by incubating the cells at RT for 30 min in a blocking solution containing 1% BSA and 0.05% Triton X-100 in PBS. The following antibodies were diluted in the blocking solution: rabbit anti-Apoa-1 (1:50, Santa Cruz Biotechnologies, Inc.). A donkey anti-rabbit IgG (H+L)-Alexa555 (1:250, Invitrogen) was used as secondary antibody and TOTO-3 (1:1500, Invitrogen) was added as a nuclear stain. Coverslips were mounted with fluorescent mounting medium (Dako), and the slides were examined using a confocal microscope (Olympus).

ELISA

c-Kit-positive cells and Ter119-positive cells were isolated by flow cytometry as described above. Proteins were extracted from the sorted cells using the Qproteome Mammalian Protein Preparation kit (Qiagen). To detect the Apoa-1 protein, a goat anti-Apoa-1 (0.8 μg/ml,

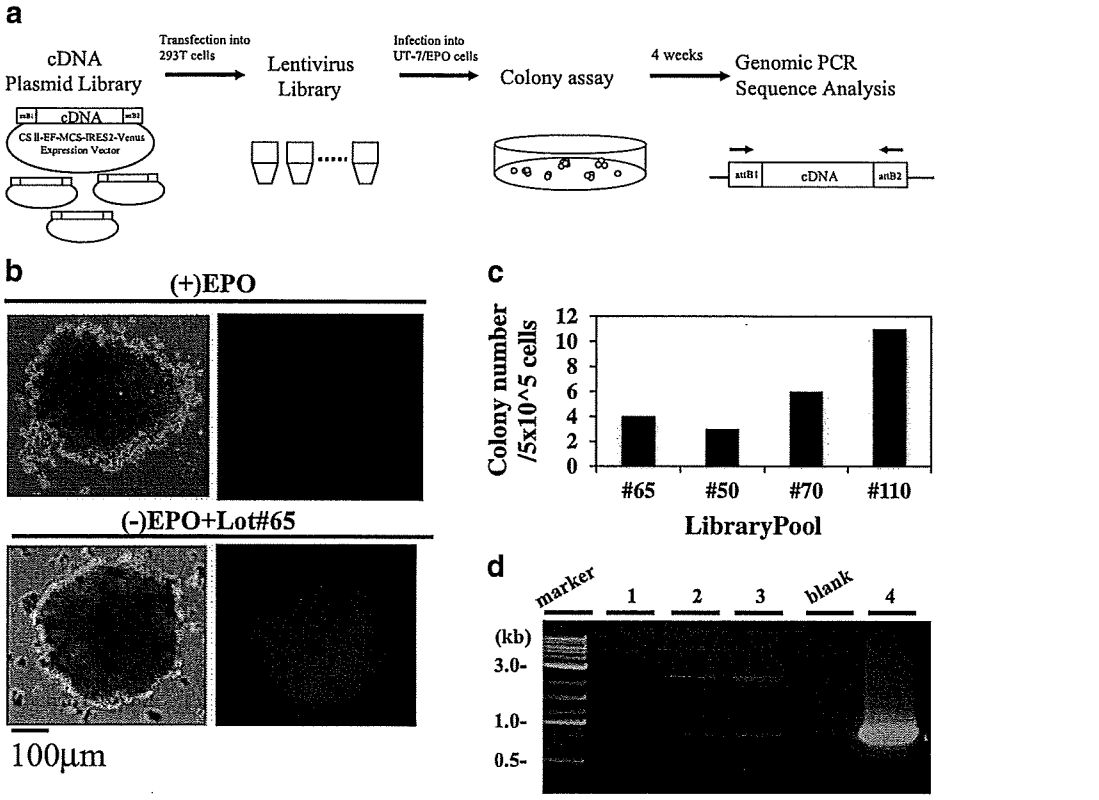

Fig. 1 Lentiviral human FL cDNA library screening in UT-7/EPO cells. **a** Strategy for identifying candidate EPO-independent regulators of erythropoiesis. Four pools (#65, #50, #70 and #110) of human FL-derived cDNA library were transfected into 293 T cells with helper plasmids to generate the lentiviral library. UT-7/EPO cells were transduced with these lentiviral library pools and then cultured in semisolid, EPO-deficient media for four weeks to positively select for clones that were able to form EPO-independent erythroid colonies. Finally, the cDNAs of the positive clones were sequenced to identify the transduced genes. **b** Erythroid colony assay. UT-7/EPO cells were transduced with the lentiviral pools (#65, #50, #70 and #110) and then transferred to semi-solid culture media. A representative colony derived from cells transduced with pool #65 is shown (Scale bar= 200 μm). A non-transduced colony was negative for Venus, while the lentiviral library-transduced colony was positive for Venus. **c** Colony number. A total of 22 colonies were obtained from UT-7/EPO cells that had been transduced with four lentiviral library pools and then analyzed by the colony formation assay. **d** Genomic PCR analysis. The inserted candidate genes were examined by genomic PCR using lentivirus insertion-specific primers. Lane 1: Untransduced UT-7/EPO cells (negative control), Lanes 2, 3: A colony derived from UT-7/EPO cells that had been transduced with lentiviral pool #65, Lane 4: GFP-transduced UT-7/EPO cells (positive control)

Rockland Immunochemicals) was used as a capture antibody, a rabbit anti-Apoa-1 (1:100, Santa Cruz Biotechnologies, Inc.,) was used as a detection antibody (primary antibody), and an anti-rabbit IgG-HRP (1:5000, Millipore) was used as the secondary antibody. Each antibody was captured onto 96-well immunoplates (Nunc) at 4°C for 16 h. Nonspecific binding was blocked by incubating the plate with 1% BSA/PBS for 2 h at RT. After the extracted proteins were added to the plate for 2 h at RT, the primary antibody was added for 1 h at RT, followed by the secondary antibody for 30 min at RT. The tetramethylbenzidine substrate was added to the wells for 30 min at RT, followed by a Stop Solution (R&D). The O.D. at 450 nm was measured using a Thermo Multiskan EX plate reader.

Results

Screening for Genes that Replace EPO/EPOR Signaling in UT-7/EPO Cells Using a Human FL Lentiviral Library

To identify novel genes that regulate erythroid cell maturation, we designed a strategy that monitored the ability of the EPO-dependent cell line, UT-7/EPO, to form erythropoietin (EPO)-independent colonies. Recently, we constructed a lentiviral human fetal liver (FL) cDNA library to search for novel genes that regulate hematopoiesis, including erythropoiesis [14]. Lentiviral cDNA library pools, which contained $1.32–1.98 \times 10^5$ cfu (colony forming units) per pool [14], were examined in this screen. We used the UT-7/EPO cell line, which is dependent upon EPO [13].

Table 1 Genes transduced in lentiviral-transduced erythroid colonies arising in the absence of Epo

Lentivirus pool #	Gene symbol	Discription
65	Angiotensinogen	AGT
	Estrogen receptor binding site associated antigen 9	EBAG9
50	B-cell CLL/lymphoma 2-like 1	BCL2-like 1
	Apolipoprotein A-1	APOA-1
70	ferritin heavy subunit	FHS
	3-phosphoinositide dependent protein kinase-1	PDPK1
	abl interactor 2	ABI-2
	Fibrinogen like 1	FGL1
	Apolipoprotein E	APOE
	Interferon induced transmembrane protein 2	1-8D
110	Asialoglycoprotein receptor 2	ASGR2
	Ferritin light chain	FLC
	Solute carrier family 27 (fatty acid transporter)	SLC27A2
	Ribosomal protein L10	RPL10
	Collagen type XVIII alpha 1	COL18A1
	Apolipoprotein J	APOJ
	Group-specific component	GC

When UT-7/EPO cells are transduced with genes in this lentiviral library that can functionally replace EPO/EPOR signaling, expression of these genes will result in colony formation in the absence of EPO (Fig. 1a). 293 T cells were transfected with four different lentiviral cDNA pools (#65, #50, #70 and #110). Subsequently, UT-7/EPO cells were transduced with these four different lentivirus library pools and cultured for four weeks in semi-solid media in the absence of EPO. Clones that acquired the ability to proliferate in the absence of EPO were identified and analyzed. Lentiviral-transduced cells were identified by Venus fluorescence that was encoded by the lentiviral vector. UT-7/EPO cells that were cultured in the absence of EPO failed to generate colonies, whereas these cells generated equal numbers of colonies when cultured in semi-solid media containing EPO (data not shown). When UT-7/EPO cells that had been transduced with the lentiviral library (6×10^5 cDNAs) were cultured in the absence of EPO, 22 EPO-independent colonies formed (Fig. 1b–c).

Next, to identify the cDNAs responsible for this EPO-independent proliferation, genomic DNA was isolated from each colony, and the integrated cDNAs were PCR amplified using lentivirus-specific primers (Fig. 1d). Agarose gel electrophoresis of the PCR products for each colony showed multiple bands of different sizes (Fig. 1d, lanes 2 and 3). This amplification was specific because untransduced UT-7/EPO cells did not yield any PCR products (lane 1), and a PCR product of the expected size was amplified from UT-7/EPO cells transduced with a lentivirus encoding green fluorescent protein (GFP) (lane 4).

Candidate Genes Identified from UT-7/EPO Cells Transduced with Human FL Lentiviral cDNA Library

The PCR products from the first round of screening were sequenced to identify the candidate genes that were expressed during erythropoiesis. Each pool contained a different number of inserted genes (Table 1). From the first screening, the following genes were identified as candidates that contributed to the growth of EPO-independent colonies; *FHS* and *FLC* encoding iron-binding proteins; the vitamin D-binding protein *GC*; the plasma protein receptor *ASGR2*; the vasoregulator *AGT*; estrogen-responsive protein *EBAG9*; the collagen *COL18A1*; the ribosomal protein *RPL10*; the kinase *PDPK1*; *ABI-2*, a kinase-binding protein; *APOA-1*, *APOE*, *APOJ* and *SLC27A2*, all of which encode lipid metabolism-related proteins; the anti-apoptotic protein *BCL2-like1*; and *1-8D*, encoding a protein of unknown function.

Among the integrated genes, some (*AGT*, *FHS*, *1-8D*, *FLC* and *GC*) were inserted into the host genome as a full-length coding sequence (CDS). As a result, these genes produced functional proteins that could be expressed in UT-7/EPO cells and lead to colony formation in the absence of EPO. Other genes (*BCL2-like1*, *APOA-1*, *PDPK1*, *FGL1*, *APOE*, *SLC27A2* and *COL18A1*) were inserted as a partial CDS that lacked the 5′ first start codons but contained 3′ stop codons, indicating that these genes were translated from a secondary start codon to the stop codon to yield partial proteins. As a result, functional proteins may be expressed in UT-7/EPO cells, leading to colony formation in the absence of EPO. The remaining inserted genes (*EBAG9*, *ABI-2*, *ASGR2* and *APOJ*) consisted of only a

Table 2 Gene specific primers for candidate genes in mice

Agt	5′	AGTGGGAGAGGTTCTCAATAGCA
	3′	GACGTGGTCGGCTGTTCCT
Ebag9	5′	GCAGCTACACAAGACATGCCTTT
	3′	TCCCACGCATTGCTATTTTCT
Bcl2-like1	5′	GGCTGGGACACTTTTGTGGAT
	3′	AAGCGCTCCTGGCCTTTC
Apoa-1	5′	GACAGCGGCAGAGACTATGTGT
	3′	AGGAGATTCAGGTTCAGCTGTTG
Fhs	5′	GCATGCCGAGAAACTGATGA
	3′	TCACGGTCTGGTTTCTTTATATCCT
Pdpk1	5′	TTCTTGGCGAGGGCTCTTT
	3′	CATATTCTCTGGAAGTGGCCAGTT
Abi-2	5′	GCGGGTGGCCGACTACT
	3′	TCTTCTAGGGCTCGCTGCTT
Apoe	5′	AGCTGCAGAGCTCCCAAGTC
	3′	TTACTTCCGTCATAGTGTCCTCCAT
1-8d	5′	CCTGGGCTTCGTTGCCTAT
	3′	CACATCGCCCACCATCTTC
Asgr2	5′	GGAGGAGAAGCAGCAACAGCTA
	3′	TGGGAAGTGCTTCAGGTGAAA
Flc	5′	CGGGCCTCCTACACCTACCT
	3′	GCCACGTCATCCCGATCA
Slc27a2	5′	CAACACACCGCAGAAACCAA
	3′	CCATTTCCCAGGGCTTTTTT
Rpl10	5′	TTCCATGTCATCCGTATCAACAA
	3′	CCCTGTCTGGAGCCTGTCA
Col18a1	5′	GCAGAGCCAGAGAATGTTGCT
	3′	CCCGACGTGAGGGTCATC
Apoj	5′	GGTCGGCCAGCAGCTAGAG
	3′	CGCCGTTCATCCAGAAGTAGA
Gc	5′	GGATCCTGCTGTACTTCTGCAA
	3′	TGCTTCATCTGGAGTCTCTCCTT

partial CDS without an open reading frame (ORF). These genes were translated from the shifted reading frame of the original mRNA and produced proteins of uncertain function. However, these genes resulted in UT-7/EPO colony formation in the absence of EPO. All of the 17 candidate cDNAs with full-length, partial or matched ORFs or partial but non-matched ORFs were examined in a secondary screen to identify specific genes that were involved in terminal erythroid maturation.

Expression of EPO-independent Growth-inducing Genes in Mouse FL Erythroid Populations

To determine which candidate genes obtained from first screen are critical for primary erythroid cell maturation, we performed a second screen to analyze gene expression during erythroid development. We used mouse fetuses for the second screen since mouse fetal samples are easier to obtain and use than human samples. The mouse homologues of these candidate genes were identified and the expression of the candidate genes was analyzed by RT-PCR using gene-specific primers (Table 2).

First, gene expression was assessed in samples from E10.5 whole embryos (WE) and E12.5 FL. All candidate genes were expressed in E12.5 FL with the exception of *Asgr-2,* which was eliminated as a gene of interest (Fig. 2). *Ebag9* and *Col18a1* expression was lower in the FL than in the whole E10.5 embryos, while *Fhs* and *Gc* had the opposite expression pattern with higher expression in the FL samples.

Next, we analyzed candidate gene expression in a series of FL-derived hematopoietic populations ranging from uncommitted hematopoietic stem cells (HSCs) to mature erythrocytes as determined by the expression of the surface markers CD45, Sca-1, c-Kit, CD71 and Ter119 (Fig. 3a). The following criteria were used to identify each hematopoietic population: (1) CD45+/Sca-1+/c-Kit+ cells represent HSCs; (2) c-Kit+ (Sca-1-/c-Kit+/CD71-/Ter119-) cells are BFU-E; (3) c-Kit+/CD71+ (Sca-1-/c-Kit+/CD71+/Ter119-) cells are committed erythroid progenitor cells or CFU-E; (4) CD71+/Ter119+ (Sca-1-/c-Kit-/CD71+/Ter119+) cells are proerythroblasts; and (5) Ter119+ (Sca-1-/c-Kit-/CD71-/Ter119+) cells represent mature erythroblasts and erythrocytes (Fig. 3a) [14, 15].

The mRNA expression of some candidate genes (*Abi-2*, *Slc27a2*) was higher in HSCs and gradually decreased throughout erythroid cell maturation (Fig. 3b). The expression of other candidate genes (*Pdpk1*, *Fhs*, *Flc*, *Rpl10*, *Ebag9* and *Apoe*) increased from HSCs to erythroblasts and then gradually decreased from erythroblasts to mature erythrocytes. *Bcl2l1* expression was low in HSCs and gradually increased. *Apoa-1* was highly expressed in

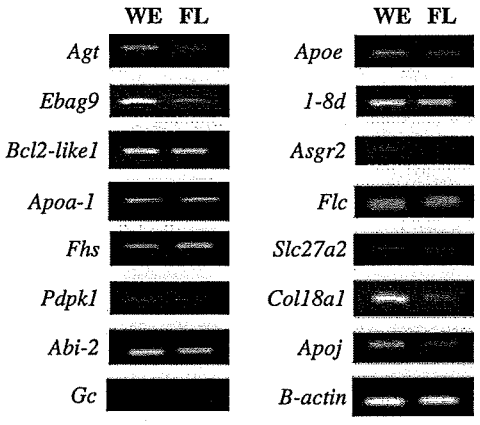

Fig. 2 Expression of candidate erythroid genes in developing mouse embryos. RT-PCR analyses of candidate genes in mouse embryos. We used RT-PCR to examine the expression patterns of the mouse homologues of each candidate gene in 10.5 dpc whole embryos (WE) and 12.5 dpc FL in ICR mouse embryos

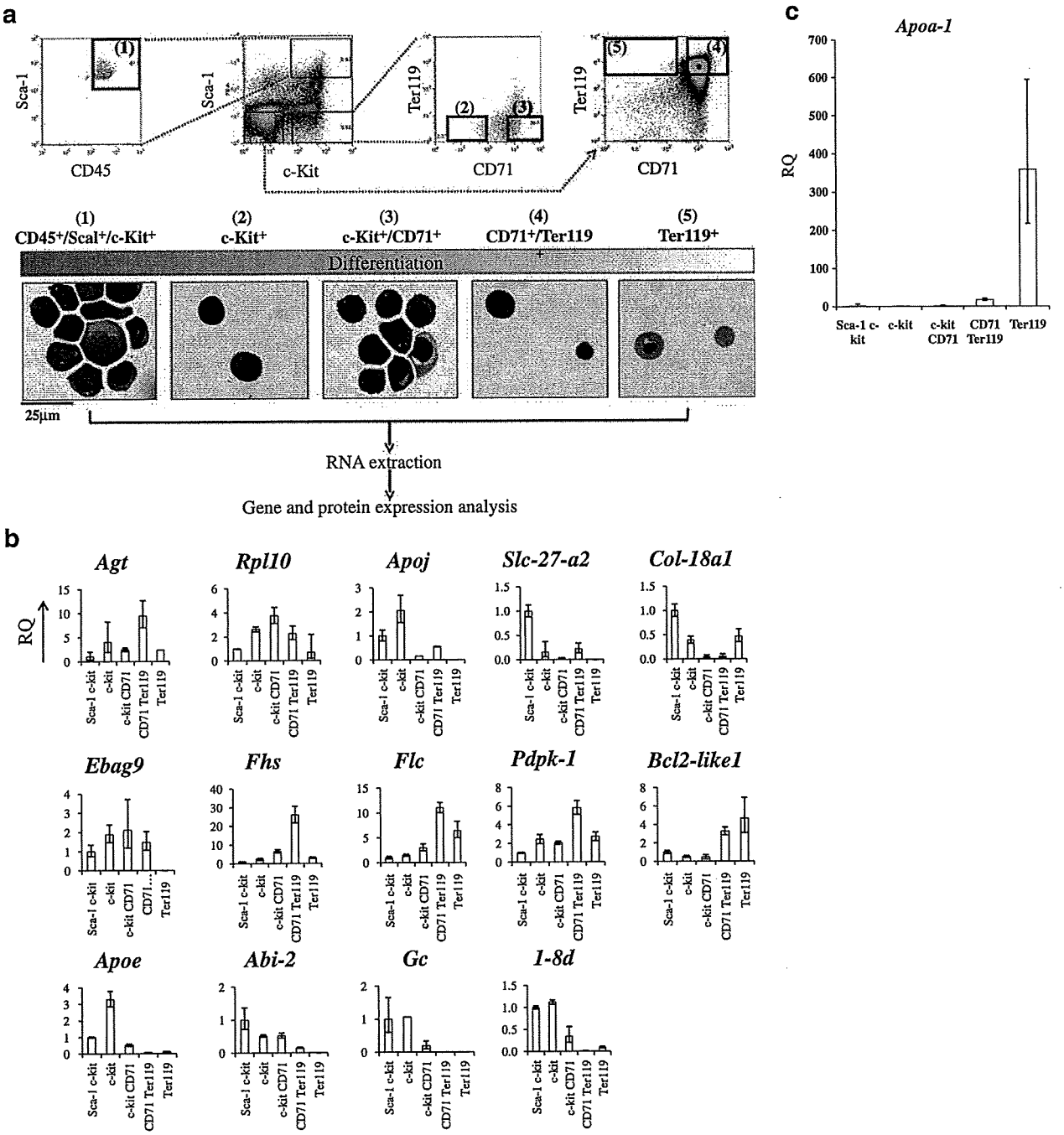

Fig. 3 Isolation of maturing erythroid populations from mouse FL cells. **a** Hematopoietic stem cells and maturing erythroid populations were isolated from 12.5 dpc mouse FL based on the expression of the surface markers CD45 (common leukocyte antigen), Sca-1 (stem cell antigen-1), c-Kit (stem cell factor receptor), CD71 (transferrin receptor) and Ter119 (Glycophorin A-associated antigen). The cytospins of each cellular fraction were prepared for May-Grunwald-Giemsa staining. As erythroid cells mature, the cell size decreased and finally the erythrocytes were enucleated. **b** mRNA expression patterns of candidate genes during erythroid cell maturation. The mRNA levels of candidate genes in maturing erythroid populations were analyzed by qRT-PCR. Total RNA was isolated from FL cells of 12.5 dpc embryos (Bars represent the means ± SD). The horizontal axes indicate the HSC fraction and the erythroid cell stage. Erythroid cell development proceeds from left to right. The vertical axes indicate the relative quantitation (RQ) of mRNA expression with the Sca-1^{+}/c-Kit^{+} cell fraction set at an RQ value of 1. **c** The expression of mouse *Apoa-1* was significantly increased in the terminal maturation stages ($Ter119^{+}$ cell fraction) of cells obtained from 12.5 dpc FL

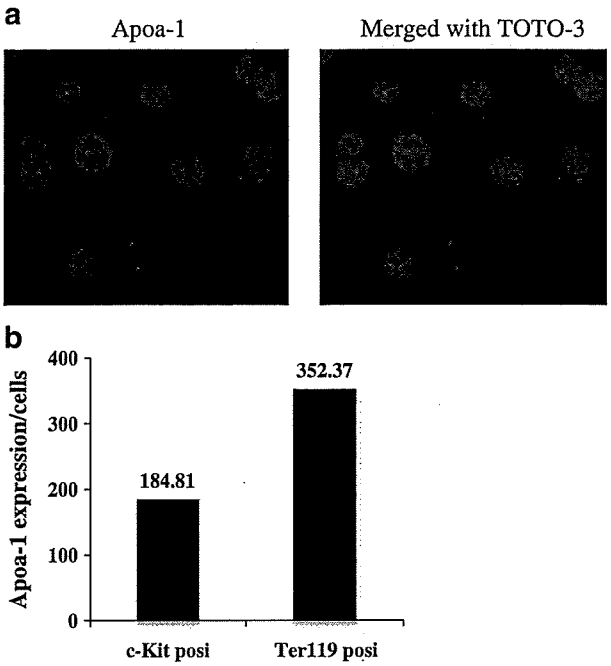

Fig. 4 Apoa-1 protein expression in mouse FL cells. **a** Immunohistochemistry. Ter119-positive cells from 12.5 dpc FL cells were cytospun and stained with an anti-mouse Apoa-1 antibody. Apoa-1-positive cells (*red*) were observed in 12.5 dpc FL cells. Nuclei were stained with TOTO3 (*blue*). **b** ELISA. c-Kit-positive cells and Ter119-positive cells from 12.5 dpc FL cells were sorted. Protein was extracted from each fraction and then analyzed by a sandwich ELISA. The expression levels of the mouse Apoa-1 proteins are shown for each fraction

Ter119-positive mature erythrocytes (Fig. 3c). The mRNA levels of *Apoa-1* increased approximately 350-fold, respectively, in the Ter119-positive cell population compared to the HSC population, suggesting that both of these genes are involved in the terminal maturation of erythroid cells.

Expression of the Apoa-1 Protein in Mouse FL Cells

To determine whether Apoa-1 is expressed at the protein level in mouse erythroid cells, immunohistochemical analyses were performed. Ter119-positive cells in mouse FL cells expressed the Apoa-1 protein (Fig. 4a). A sandwich enzyme-liked immunosorbent assay (ELISA) was also performed to quantitatively analyze the protein expression level in 12.5 dpc mouse FL cells. Because it is difficult to extract sufficient amounts of protein for an ELISA from individually fractionated cells in the populations shown in Fig. 3a, we compared the following two groups to analyze protein expression: c-Kit-positive cells, namely ((1)+(2)+(3) in Fig. 3) and Ter119-positive cells or ((4)+(5) in Fig. 3). As shown in Fig. 4b, Apoa-1 protein expression was approximately two-fold higher in Ter119-positive cells than c-Kit-positive cells, indicating that Apoa-1 expression correlates with terminal erythroid maturation at the protein level.

APOA-1 Expression in Human Peripheral Blood

To determine whether APOA-1 is useful as a terminal erythroid marker in human samples, we examined mRNA

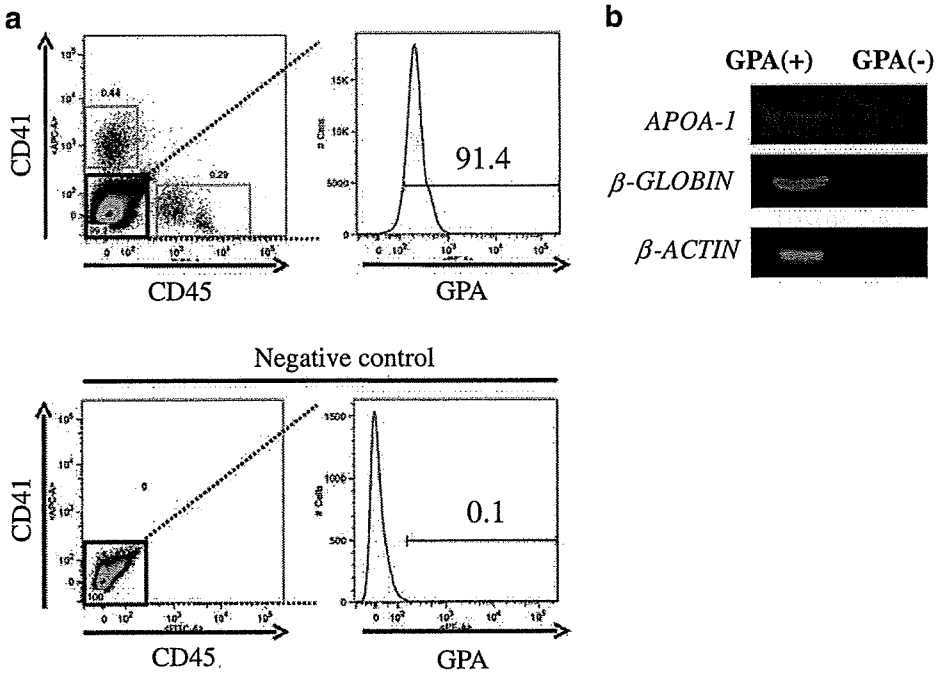

Fig. 5 *APOA-1* gene expression in human peripheral blood. **a** Erythrocytes and reticulocytes were isolated from human peripheral blood based on the expression of surface markers CD41 (integrin IIb), CD45 (common leukocyte antigen) and GPA (glycophorin A). **b** RT-PCR was performed to assess expression of human *APOA-1*. Human *β-GLOBIN* expression was analyzed to confirm that erythrocytes and reticulocytes had been isolated by flowcytometry. *APOA-1* was expressed in human peripheral blood

expression in human peripheral blood (PB) erythrocytes and reticulocytes. Erythrocytes and reticulocytes were isolated from peripheral blood by flow cytometry based on the expression of the cell surface markers glycophorin A (GPA), CD41 and CD45. In the PB, 91.4% of the CD41-/CD45-cells were positive for GPA (Fig. 5a). Reverse transcriptase PCR (RT-PCR) analysis showed that *β-GLOBIN* was expressed in GPA-positive cells, indicating that erythrocyte and reticulocyte mRNA was successfully extracted from the PB (Fig. 5b). Furthermore, *APOA-1* mRNA was expressed in the same fraction, demonstrating that this molecules can be used as a potential marker for terminal erythroid maturation in humans as well as mice.

Discussion

The goal of this study was to identify novel genes that are expressed during the terminal, EPO-independent maturation of erythroid cells. A two-step approach consisting of a lentiviral human FL cDNA library screen followed by an analysis of the gene expression patterns during erythropoiesis was performed to efficiently identify target genes.

This strategy had two clear advantages. First, it is important to establish a screening system that can detect erythropoiesis-related genes in an EPO-independent manner. A human FL cDNA library can be screened to identify novel genes. In this study, UT-7/EPO cells were transduced with a FL cDNA expression lentiviral library to detect genes that generate erythroid colonies in semi-solid medium in the absence of the EPO signaling pathway. Second, this screen could examine the effects of a large number (6×10^5) of genes on erythroid maturation. As humans are estimated to have approximately $2–3\times10^4$ genes, our screening encompassed a sufficient number of human cDNAs.

BCL2-like1 (BCL2L1) was one of the candidate genes identified in the first screen. *BCL2L1* encodes an anti-apoptotic protein that plays an important role in erythropoiesis in the absence of EPO [16]. Therefore, the results of our first screen strongly indicated that this system could be used to identify EPO-independent erythropoiesis-related genes. Other candidate genes included *FHS* and *FLC*, which encode iron-binding proteins, and *APOE, APOA-1, APOJ* and *SLC27A2,* which encode lipid metabolism-related proteins. Both iron and lipid metabolism are important cellular processes that regulate erythroid maturation [17–19]. We also identified a number of genes that were not previously implicated in erythropoiesis, including a vitamin D-binding protein (*GC*), vasoregulator (*AGT*), estrogen-responsive gene (*EBAG9*), collagen type 18 (*COL18A1*), ribosomal protein (*RPL10*) and several kinase-related proteins (*PDPK1* and *ABI-2*).

We also specifically identified a gene that was upregulated in the terminal stages of erythrocyte maturation. The identification of this gene is significant because very few molecular markers can be used to examine this stage of erythropoiesis. The candidate gene, *APOA-1*, was particularly interesting. APOA-1 is a major protein component of high-density lipoprotein (HDL) in the plasma and promotes the efflux of cholesterol from the tissues to the liver for excretion [20]. APOA-1 is a cofactor for lecithin cholesterol acyltransferase (LCAT), which is responsible for the formation of most plasma cholesteryl esters.

APOA-1 interacts with the ATP-binding cassette transporter ABCA1 (member 1 of human transporter sub-family ABCA) [21]. A recent report demonstrated that the APOA-1/ABCA1 pathway functions as an anti-inflammatory receptor by activating Janus Kinase 2 (JAK2)/Signal Transducers and Activation of Transcription3 (STAT3) in macrophages [22]. JAK2/STAT3 and/or JAK2/STAT5 are central signal pathways in erythroid cells [23]. Therefore, APOA-1/ABCA1 may activate the JAK2/STAT3 and/or JAK2/STAT5 pathway during the terminal maturation of erythroid cells.

It is intriguing to note that defects in APOA-1 are associated with low HDL levels observed in HDL deficiency type 1, which includes analphalipoproteinemia or Tangier disease. In Tangier disease patients, APOA-1 fails to associate with HDL. This inability to bind HDL is likely due to the faulty conversion of pro-APOA-1 molecules into mature chains, either due to a defect in the converting enzyme or a specific structural defect [24–26]. Furthermore, red blood cells in patients with Tangier disease have stomatocytosis and hemolytic anemia [27]. Moreover, patients with beta-thalassemia major as well as sickle cell disease have lower levels of APOA-1 in their plasma than healthy controls [28]. This abnormal erythrocyte morphology could be partially explained by a recent report by Holm TM et al., which showed that knockout mice with defects in the high-density lipoprotein receptor SR-BI have abnormal erythrocyte morphology. On the other hand, the fractional catabolic rate (FCR) for APOA-1 was significantly increased in patients with myeloproliferative disorders, including polycythemia vera, compared with healthy controls [29]. Therefore, accelerated red blood cell production could be also supported by increased APOA-1 catabolism. Further studies including both in vitro and/or in vivo analyses of APOA-1 knockouts are necessary to demonstrate the direct importance of APOA-1 in the maturation of red blood cells.

This study is the first to report that APOA-1 is a novel molecular marker for terminal erythroid maturation from HSC. In combination with Ter119 antigen or glycophorin A antigen, this molecule can potentially be used to identify mature erythrocytes in in vitro cultured erythroid cell

sources such as ES or iPS cells. It will be necessary to further investigate whether APOA-1 plays pivotal roles in erythroid cell maturation and is a useful maturation marker.

Acknowledgements The authors would like to thank Chiyo Mizuochi, Yuka Horio, Tatsuya Sasaki and Michiko Ushijima at Kyushu University for excellent technical assistance. This work was supported by a grant from the Project for Realization of Regenerative Medicine from the Ministry of Education, Culture, Sports, Science and Technology and by a grant from the BASIS project from the Ministry of Education, Culture, Sports, Science and Technology. T. Inoue is supported by research fellowships from the Japan Society for the Promotion of Science for Young Scientists.

Disclosures The authors indicate no potential conflicts of interest.

References

1. Weissman, I. L. (2000). Stem cells: units of development, units of regeneration, and units in evolution. *Cell, 100*, 157–168.
2. Mikkola, H. K., & Orkin, S. H. (2006). The journey of developing hematopoietic stem cells. *Development, 133*, 3733–3744.
3. Medvinsky, A., & Dzierzak, E. (1996). Definitive hematopoiesis is autonomously initiated by the AGM region. *Cell, 86*, 897–906.
4. Sugiyama, D., & Tsuji, K. (2006). Definitive hematopoiesis from endothelial cells in the mouse embryo; a simple guide. *Trends in Cardiovascular Medicine, 16*, 45–49.
5. Ema, H., & Nakauchi, H. (2000). Expansion of hematopoietic stem cells in the developing liver of a mouse embryo. *Blood, 95*, 2284–2288.
6. Palis, J. (2008). Ontogeny of erythropoiesis. *Current Opinion in Hematology, 15*, 155–161.
7. McGrath, K., & Palis, J. (2008). Ontogeny of erythropoiesis in the mammalian embryo. *Current Topics in Developmental Biology, 82*, 1–22.
8. Hiroyama, T., Miharada, K., Sudo, K., Danjo, I., Aoki, N., & Nakamura, Y. (2008). Establishment of mouse embryonic stem cell-derived erythroid progenitor cell lines able to produce functional red blood cells. *PLos One, 3*, e1544.
9. Kina, T., Ikuta, K., Takayama, E., et al. (2000). The monoclonal antibody TER-119 recognizes a molecule associated with glycophorin A and specifically marks the late stages of murine erythroid lineage. *British Journal Haematology, 109*, 280–287.
10. Zhang, J., Socolovsky, M., Gross, A. W., & Lodish, H. F. (2003). Role of Ras signaling in erythroid differentiation of mouse fetal liver cells: functional analysis by a flow cytometry-based novel culture system. *Blood, 102*, 3938–3946.
11. Kurita, R., Sasaki, E., Yokoo, T., et al. (2006). Tal1/Scl gene transduction using a lentiviral vector stimulates highly efficient hematopoietic cell differentiation from common marmoset (Callithrix jacchus) embryonic stem cells. *Stem Cells, 24*, 2014–2022.
12. Kurita, R., Oikawa, T., Okada, M., et al. (2008). Construction of a high-performance human fetal liver-derived lentiviral cDNA library. *Molecular and Cellular Biochemistry, 319*, 181–187.
13. Komatsu, N., Yamamoto, M., Fujita, H., et al. (1993). Establishment and characterization of an erythropoietin-dependent subline, UT-7/Epo, derived from human leukemia cell line, UT-7. *Blood, 82*, 456–464.
14. Suzuki, N., Suwabe, N., Ohneda, O., et al. (2003). Identification and characterization of 2 types of erythroid progenitors that express GATA-1 at distinct levels. *Blood, 102*, 3575–3583.
15. Walkley, C. R., & Orkin, S. H. (2006). Rb is dispensable for self-renewal and multilineage differentiation of adult hematopoietic stem cells. *Proceedings of the National Academy of Sciences of the United States of America, 103*, 9057–9062.
16. Dolznig, H., Habermann, B., Stangl, K., et al. (2002). Apoptosis protection by the Epo target Bcl-X(L) allows factor-independent differentiation of primary erythroblasts. *Current Biology, 12*, 1076–1085.
17. Gelvan, D., Fibach, E., Meyron-Holtz, E. G., & Konijn, A. M. (1996). Ferritin uptake by human erythroid precursors is a regulated iron uptake pathway. *Blood, 88*, 3200–3207.
18. Meyron-Holtz, E. G., Vaisman, B., Cabantchik, Z. I., et al. (1999). Regulation of intracellular iron metabolism in human erythroid precursors by internalized extracellular ferritin. *Blood, 94*, 3205–3211.
19. Holm, T. M., Braun, A., Trigatti, B. L., et al. (2002). Failure of red blood cell maturation in mice with defects in the high-density lipoprotein receptor SR-BI. *Blood, 99*, 1817–1824.
20. Breslow, J. L., Ross, D., McPherson, J., et al. (1982). Isolation and characterization of cDNA clones for human apolipoprotein A-I. *Proceedings of the National Academy of Sciences of the United States of America, 79*, 6861–6865.
21. Fitzgerald, M. L., Morris, A. L., Rhee, J. S., Andersson, L. P., Mendez, A. J., & Freeman, M. W. (2002). Naturally occurring mutations in the largest extracellular loops of ABCA1 can disrupt its direct interaction with apolipoprotein A-I. *Journal of Biological Chemistry, 277*, 33178–33187.
22. Tang, C., Liu, Y., Kessler, P. S., Vaughan, A. M., & Oram, J. F. (2009). The macrophage cholesterol exporter ABCA1 functions as an anti-inflammatory receptor. *Journal of Biological Chemistry, 47*, 32336–32343.
23. Richmond, T. D., Chohan, M., & Barber, D. L. (2005). Turning cells red: signal transduction mediated by erythropoietin. *Trends in Cell Biology, 15*, 146–155.
24. Zannis, V. I., Lees, A. M., Lees, R. S., & Breslow, J. L. (1982). Abnormal apoprotein A-I isoprotein composition in patients with Tangier disease. *Journal of Biological Chemistry, 257*, 4978–4986.
25. Gordon, J. I., Sims, H. F., Lentz, S. R., Edelstein, C., Scanu, A. M., & Strauss, A. W. (1983). Proteolytic processing of human preproapolipoprotein A-I. A proposed defect in the conversion of pro A-I to A-I in Tangier's disease. *Journal of Biological Chemistry, 258*, 4037–4044.
26. Schmitz, G., Assmann, G., Rall, S. C., Jr., & Mahley, R. W. (1983). Tangier disease: defective recombination of a specific Tangier apolipoprotein A-I isoform (pro-apo A-i) with high density lipoproteins. *Proceedings of the National Academy of Sciences of the United States of America, 80*, 6081–6085.
27. Reinhart, W. H., Gossi, U., Butikofer, P., et al. (1989). Haemolytic anaemia in analpha-lipoproteinaemia (Tangier disease): morphological, biochemical, and biophysical properties of the red blood cell. *British Journal Haematology, 72*, 272–277.
28. Sasaki, J., Waterman, M. R., & Cottam, G. L. (1986). Decreased apolipoprotein A-I and B content in plasma of individuals with sickle cell anemia. *Clinical Chemistry, 32*, 226–227.
29. Ginsberg, H. N., Le, N. A., & Gilbert, H. S. (1986). Altered high density lipoprotein metabolism in patients with myeloproliferative disorders and hypocholesterolemia. *Metabolism, 35*, 878–882.

jgm1467

RESEARCH ARTICLE

THE JOURNAL OF GENE MEDICINE
J Gene Med 2010; **12**: 000–000.
Published online in Wiley InterScience (www.interscience.wiley.com) **DOI:** 10.1002/jgm.1467

Carrier cell-mediated cell lysis of squamous cell carcinoma cells by squamous cell carcinoma antigen 1 promoter-driven oncolytic adenovirus

Katsuyuki Hamada[1]*
Ting Zhang[2]
Junzo Desaki[3]
Koh-ichi Nakashiro[2]
Hiroshi Ito[4]
Kenzaburo Tani[5]
Yoshiyuki Koyama[6]
Hiroyuki Hamakawa[2]

[1]*Department of Obstetrics and Gynecology, Ehime University, Ehime, Japan*

[2]*Department of Oral and Maxillofacial Surgery, Ehime University, Ehime, Japan*

[3]*Department of Anatomy, Ehime University, Ehime, Japan*

[4]*Animal Medical Center, Tokyo University of Agriculture and Technology, Tokyo, Japan*

[5]*Department of Advanced Molecular and Cell Therapy, Kyushu University Hospital, Kyushu University, Fukuoka, Japan*

[6]*Department of Textile Science, Otsuma Women's University, Tokyo, Japan*

*Correspondence to:
Katsuyuki Hamada, Department of Obstetrics and Gynecology, School of Medicine, Ehime University, Shitsukawa, Toon, Ehime 791-0295, Japan.
E-mail: hamakatu@m.ehime-u.ac.jp

Received: 5 October 2009
Revised: 1 February 2010
Accepted: 27 April 2010

Abstract

Background The squamous cell carcinoma antigen (SCCA) serves as a serological marker for squamous cell carcinomas. Molecular cloning of the *SCCA* genomic region has revealed the presence of two tandemly arrayed genes: *SCCA1* and *SCCA2*. *SCCA1* gene is up-regulated in squamous cell carcinoma cells. We analyzed the proximal region of the *SCCA1* promoter and the antitumor effect of oncolytic adenovirus driven by the *SCCA1* promoter in squamous cell carcinoma cells.

Methods The *SCCA1* promoter was analyzed by dual luciferase assay and substituted with the *E1A* promoter to construct the oncolytic adenovirus to determine the squamous cell carcinoma-specific cell lysis.

Results Deletion analysis of *SCCA1* promoter identified a 175-bp core promoter region and an enhancer region at −525 to −475 bp upstream of the transcription start site. The transcriptional activity of the *SCCA1* promoter was up-regulated in squamous cell carcinoma cells. Five tandem repeats of enhancer increased *SCCA1* promoter activity by four-fold. Oncolytic adenovirus driven by this *SCCA1* enhancer-promoter complex specifically killed squamous cell carcinoma cells *in vitro* and *in vivo*. A549 carrier cells infected with the oncolytic adenovirus induced complete regression of syngeneic squamous cell carcinoma cell tumor by overcoming immunogenicity and adenovirus-*mGM-CSF* augmented the antitumor effect of carrier cells.

Conclusions *SCCA1* was up-regulated in squamous cell carcinoma cells and oncolytic adenovirus driven by *SCCA1* promoter specifically killed these cells. These findings suggest that *SCCA1* promoter is a potential target of gene therapy for squamous cell carcinoma. Copyright © 2010 John Wiley & Sons, Ltd.

Keywords adenovirus; cervical cancer; oncolytic carrier cell; promoter; squamous cell carcinoma; squamous cell carcinoma antigen 1

Introduction

Squamous cell carcinoma antigen (SCCA) is a circulating tumor marker for squamous cell carcinoma, especially that of cervix, head and neck, lung, and oesophagus [1]. Elevated circulating levels of SCCA are not detected in patients with adenocarcinomas of the uterus, ovary, or breast [2]. Several studies have shown that increased serum SCCA levels are correlated with the extent of disease in patients with squamous cell carcinoma [2–4]. Higher

SCCA levels are also indicative of deep tumor infiltration and lymph node involvement [5,6]. Moreover, measurement of post-treatment SCCA levels is useful for monitoring the response to therapy as well as for predicting tumor recurrence and metastasis. SCCA protein has been isolated from a metastatic, cervical squamous cell carcinoma [2]. Molecular cloning of the *SCCA* genomic region revealed the presence of two tandemly arrayed genes: *SCCA1* and *SCCA2*. Although SCCA1 and SCCA2 are almost identical members of the serpin superfamily, the significant differences in their reactive site loops suggest that SCCA1 is a papain-like cysteine proteinase inhibitor, whereas SCCA2 is a chymotrypsin-like serine proteinase inhibitor [7].

Previous studies have reported the cloning and characterization of the promoter region of *SCCA1* [8] and *SCCA2* [9]. *SCCA1* gene expression and promoter activity is up-regulated in squamous cell carcinoma cells compared to keratinocyte and adenocarcinoma cells [8,10]. *SCCA2* gene expression and promoter activity are also increased in squamous cell carcinoma cells compared to normal and adenocarcinoma cells, although the *SCCA1* gene expression and promoter activity are higher than the *SCCA2* gene expression in almost all squamous carcinoma cells and tissues [8,10]. These findings suggest that *SCCA1* promoter may be a potential target of gene therapy for squamous cell carcinoma. Although the *SCCA2* promoter has been introduced into E1-deleted adenovirus to transduce an apoptotic gene in lung cancer [11], use of *SCCA1* promoter-driven adenovirus to treat squamous cell carcinoma has not yet been reported. We found that up to five consecutive tandem-repeat enhancer elements significantly increased *SCCA1* promoter activity. Oncolytic adenovirus AdE3-*SCCA1* was constructed by replacement of adenovirus *E1A* promoter with this tandem-repeat enhancer and promoter complex and specifically killed squamous cell carcinoma cells.

Materials and methods

Cell lines and culture conditions

Human non-small cell lung cancer A549, cervical squamous cell carcinoma SKGIIIa and gastric cancer AGS cells were obtained from the Japanese Collection of Research Bioresources Cell Bank (Osaka, Japan). Human ovarian carcinoma HEY and 2774 cells were obtained from Dr G. Mills, murine squamous cell carcinoma SCC7 cells were obtained from Dr L. Milas, and human non-small cell lung cancer H1299 cells were obtained from Dr J. A. Roth (The University of Texas, MD Anderson Cancer Center, TX, USA). Normal human keratinocyte SV, HPK, NHK and K42 cells and normal human fibroblast F27 cells were established by Dr K. Hashimoto (Ehime University, Japan). Normal human fibroblast NF and ovarian fibroblast NOE cells were established in our laboratory. Human umbilical vein endothelial HUVEC cells was obtained from Cambrex Bio Science Walkersville Inc. (Walkersville, MD, USA). Human cervical squamous cell carcinoma HT-III, C4I, C4II and CaSki cells, and human cervical adenocarcinoma HeLa cells, were obtained from the American Type Culture Collection (Rockville, MD, USA).

Cells were maintained in a humidified 5% CO_2/95% air incubator at 37 °C. All cell lines, except NHK, K42 and HUVEC cells, were grown in RPMI medium supplemented with 10% heat-inactivated fetal bovine serum. NHK and K42 cells were grown in MCDB153 (Nissui Co., Tokyo, Japan) with bovine hypothalamus extract. HUVEC cells were grown in EBM-2 (Cambrex, Baltimore, MD, USA)

Construction of the AdE3-*SCCA1* vector

The pXC1 plasmid has adenovirus 5 sequences from nucleotides 22–5790 containing the *E1* gene (Microbix Biosystems Inc., Toronto, Canada). A unique *AgeI* site was introduced at nucleotide position 404 after deletion between nucleotides 404 and 552 to generate the plasmid pXC1-404-*AgeI*. The *SCCA1* promoter was ligated to pXC1-404-*AgeI* plasmid to obtain pXC1-*SCCA1*. To construct the AdE3-*SCCA1* virus, homologous recombination was performed between pXC1-*SCCA1* plasmid and the right hand side of pBHGE3 adenovirus DNA containing the *E3* region in 293 cells by a standard technique [12]. To construct the wild-type adenovirus AdE3, homologous recombination was performed between pXC1 and pBHGE3 in 293 cells. The replication defective *E1*-deleted Ad5CMV-*LacZ* virus was used as control adenovirus. All viruses were purified with double CsCl gradients using standard methods, and titered by standard spectrophotometry and plaque assay [12].

Enzyme-linked immunosorbent assay (ELISA)

Each cell was seeded at 4×10^6 cells into 100-mm culture dishes and incubated for 2 days with 10 ml of culture medium. Each cell line was cultured in triplicate dishes. Supernatants were obtained from culture medium in each dish, centrifuged for 5 min at 3000 r.p.•m. at room temperature, and assayed to detect SCCA protein. An ELISA for SCCA (IMx SCC.•DAINAPACK™; Dainabot Co., Tokyo, Japan) was used to evaluate the concentrations of SCCA protein in medium. Medium samples (2 ml) were concentrated ten-fold by centrifugation with a Centricon-10 (Millipore Corp., Bedford, MA, USA). Concentrated samples (200 µl) were applied to an automatic assay apparatus (IMx analyzer; Dainabot Co.). The lower limit of detection with this ELISA system was 0.01 ng/ml. This assay system could detect both SCCA1 and SCCA2 proteins. The mean values of samples were determined in triplicates. All experiments were performed at least three times and gave similar results.

Real-time quantitative reverse transcriptase-polymerase chain reaction (RT-PCR)

One hundred ng RNA samples were used in RT and real-time PCR for RNA expression studies. A reverse transcriptase and real-time PCR reaction was carried out with the ABI prism 7700 sequence detection system (Applied Biosystems, Foster City, CA, USA) in a total volume of 50 µl that contained TaqMan one step RT-PCR master mix (Applied Biosystems), 0.3 µM of each forward and reverse primer, and 0.21 µM of MGB probe. The forward and reverse primer and MGB probe were: 5′-CCACCGCTGTAGTAGGATTCG-3′, 5′-GGAAAGGGTGATTACAATGGAACTC-3′ and 5′-ATCATCACCTACTTCAAC-3′ for *SCCA1* and 5′-CATGACC TGGAGCCACGG-3′, 5′-CCCTCCTCAGTGACCTCCAC-3′ and 5′-CTCTCAGTATCTAAAGTCCTAC-3′ for *SCCA2*. The reaction was performed with the following thermal cycling method: 30 min at 48 °C for reverse transcription, 5 min at 95 °C for AmpliTaq Gold activation, 15 s at 95 °C and 60 s at 60 °C for 40 cycles. *GAPDH* was chosen as a housekeeping gene to be tested as an endogenous control.

Assay for promoter activity

SCCA1 and *SCCA2* promoter fragments were inserted into the luciferase reporter vector PicaGene Basic, a promoterless and enhancerless vector (Toyo Ink MFG Co., Tokyo, Japan). The sequence of each insert was confirmed by an ABI PRISM 310 Genetic Analyzer (Applied Biosystems). Constructs containing *SCCA1* and *SCCA2* promoter sequences were fused to the *Luciferase* gene which were transfected into cells in the presence of Lipofectamine transfection reagent (Invitrogen, Carisbad, CA, USA), in accordance with manufacturer's instructions. Briefly, 1×10^5 cells seeded in a 12-well culture dish were exposed to transfection mixtures containing 1 µg of luciferase reporter plasmids and 0.2 µg of prenilla luciferase-herpes simplex virus thymidine kinase promoter control vector (Promega, Madison, WI, USA) at 37 °C for 48 h. Dual luciferase assays were performed in accordance with manufacturer's instructions.

Cell count assay

Cells were plated at a density of 5×10^3 cells/well in 12-well plates. Cells were infected with AdE3-*SCCA1* or AdE3. Culture medium alone was used as a mock infection control. After 15 days, cells were harvested and counted to determine the 50% growth inhibitory concentration (IC_{50}).

Inhibition of subcutaneous tumor growth *in vivo*

To determine inhibition of xenograftic subcutaneous tumor growth, AdE3-*SCCA1* was injected into subcutaneous tumors in female nude (*nu/nu*) mice (CLEA Japan Inc., Tokyo, Japan). In brief, 1×10^7 HT-III or H1299 cells in 100 µl of RPMI were injected into the left posterior flank of each mouse through an insulin syringe with a 27 1/2-gauge needle. Ten animals were used for each group. After 25 days, tumors with a diameter of 5–8 mm were established. Then 100 µl of AdE3 [1×10^{10} plaque-forming units (PFU)], AdE3-*SCCA1* (1×10^{10} PFU), Ad5CMV-*LacZ* (1×10^{10} PFU), or medium alone was injected intratumorally on days 0, 1, 2, 3, 4 and 5. The tumors were measured every 5 days with calipers in two perpendicular diameters. Tumor volume was calculated by assuming a spherical shape, with the average tumor diameter calculated as the square root of the product of cross-sectional diameters.

To determine inhibition of syngeneic subcutaneous tumor growth, murine SCC7 cells (1×10^6) were injected into the left posterior flank of female C3H/HeN mice (CLEA Japan Inc.) and AdE3-*SCCA1* was injected into subcutaneous tumors. Ten animals were used for each group. Medium alone; AdE3-*SCCA1* (1×10^{10} PFU) or A549 carrier cells (5×10^6) infected with AdE3-*SCCA1* at a multiplicity of infection (MOI) of 200; A549 carrier cells (5×10^6) infected with AdE3-*SCCA1* at a MOI of 200; and AxCA*mGM-CSF* at a MOI of 10 were injected into the tumors (5–8 mm in diameter) on days 0, 1 and 2. Mice were preimmunized with Ad-*LacZ* (1×10^{10} PFU) on day -21.

Animal studies have been approved by the Ehime University Review Board.

Statistical analysis

Values are the mean ± SD, and were examined with the unpaired *t*-test, Welch test and regression analysis. Survival data were plotted on Kaplan–Meier curves and examined with the log-rank test using the LIFETEST •procedure. $p < 0.05$ was considered statistically significant.

Results

Expression of SCCA protein

To determine the levels of expression of SCCA protein in human cervical squamous cell carcinoma cells, ELISA was performed in the medium of each cell line. SKGIIIa and HT-III cells secreted the highest concentrations of SCCA proteins into medium (Figure 1). The mean level of SCCA protein secretion by cervical squamous cell carcinoma cells was 15-fold greater than that of keratinocyte cells, 404-fold greater than that of normal non-keratinocyte

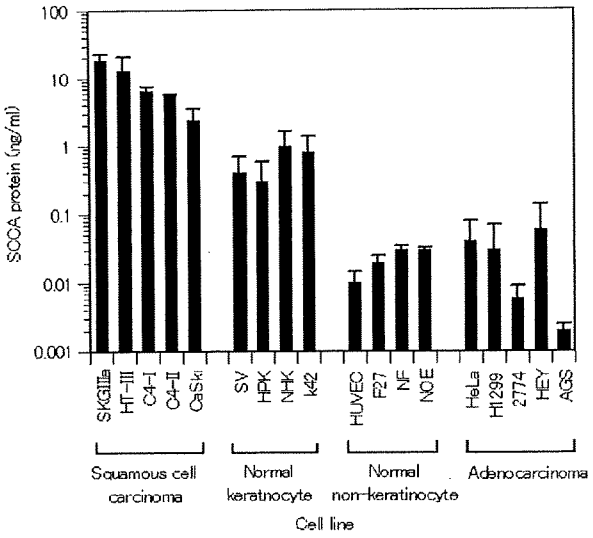

Figure 1. SCCA protein levels determined by ELISA in cervical squamous cell carcinoma, normal keratinocyte, normal non-keratinocyte and adenocarcinoma cells

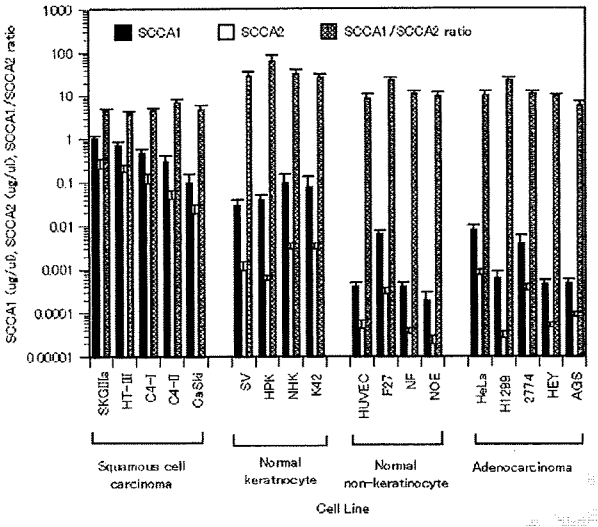

Figure 2. *SCCA1* and *SCCA2* mRNA levels determined by real time RT-PCR in cervical squamous cell carcinoma, normal keratinocyte, normal non-keratinocyte and adenocarcinoma cells

cells and 329-fold greater than that of adenocarcinoma cells. The mean level of SCCA protein secretion by keratinocyte cells was 28-fold greater than that of normal non-keratinocyte cells and 23-fold greater than that of adenocarcinoma cells. The mean level of SCCA protein secretion by normal non-keratinocyte cells was not significantly different from that of adenocarcinoma cells.

mRNA levels of *SCCA1* and *SCCA2* in cervical squamous cell carcinoma cells

To examine the mRNA levels of *SCCA1* and *SCCA2* in cervical squamous cell carcinoma cells, one-step real time RT-PCR was performed using MGB probe. The mRNA level of *SCCA1* was one or two orders of magnitude higher than that of *SCCA2* in all cell types examined (Figure 2). The mRNA level of *SCCA1* in cervical squamous cell carcinoma cells was 8.5-, 280- and 195-fold greater than that in normal keratinocytes, normal non-keratinocytes and adenocarcinoma cells, respectively. The mRNA level of *SCCA1* in normal keratinocyte cells was 33- and 23-fold greater than that in normal non-keratinocytes and adenocarcinoma cells, respectively. The mRNA level of *SCCA1* in normal non-keratinocyte cells was not significantly different from that in adenocarcinoma cells.

Transcriptional activities of *SCCA1* and *SCCA2* in squamous cell carcinoma cells

To examine the transcriptional activities of *SCCA1* in squamous cell carcinoma cells, transient expression assays were performed. Luciferase reporter plasmids containing varying lengths of the 5′-flanking regions of the gene were constructed (SCCA1-750, SCCA1-550, SCCA1-525, SCCA1-500, SCCA1-475, SCCA1-450, SCCA1-375, SCCA1-250, SCCA1-175, SCCA1-125 and SCCA1-75) as shown in Figure 3A and transfected into HT-III cells, and cell lysates were tested in luciferase assays. Figure 3B demonstrates the transcriptional activities in HT-III cells. Deletion analysis from the −750-bp to −525-bp region upstream from the gene revealed a gradual increase in transcriptional activity with a decrease in length, suggesting the presence of a sequence inhibiting transcriptional activities of the gene between −750-bp and −525-bp. A region from −525-bp to −475-bp of the *SCCA1* promoter demonstrated significant transcriptional activity. Deletion analysis from the −450-bp to −175-bp region upstream from the gene revealed a gradual increase in transcriptional activity with a decrease in length of promoter, suggesting the presence of a sequence inhibiting transcriptional activities of the gene between −450-bp and −250-bp. A −175-bp region of the *SCCA1* promoter demonstrated significant transcriptional activity. This proximal negative region from −525-bp to −475-bp and the positive −175-bp region have not been reported previously [8].

To determine the enhancer region, the intron 1 region or proximal promoter region from −525-bp to −475-bp was inserted upstream of the −175-bp region of *SCCA1* luciferase promoter plasmid. Luciferase reporter plasmids of SCCA1-175 containing intron 1 in sense or antisense orientation or the region from −525-bp to −475-bp were constructed (INT-SCCA1-175 for sense orientation of intron 1, INT-AS-SCCA1-175 for antisense orientation of intron 1, 525-SCCA1-175 for sense orientation of −525-bp to −475-bp, 525-AS-SCCA1-175 for antisense orientation of −525-bp to −475-bp, and 525-2-SCCA1-175, 525-3-SCCA1-175, 525-4-SCCA1-175, 525-5-SCCA1-175, 525-10-SCCA1-175 and 525-20-SCCA1-175 for tandem

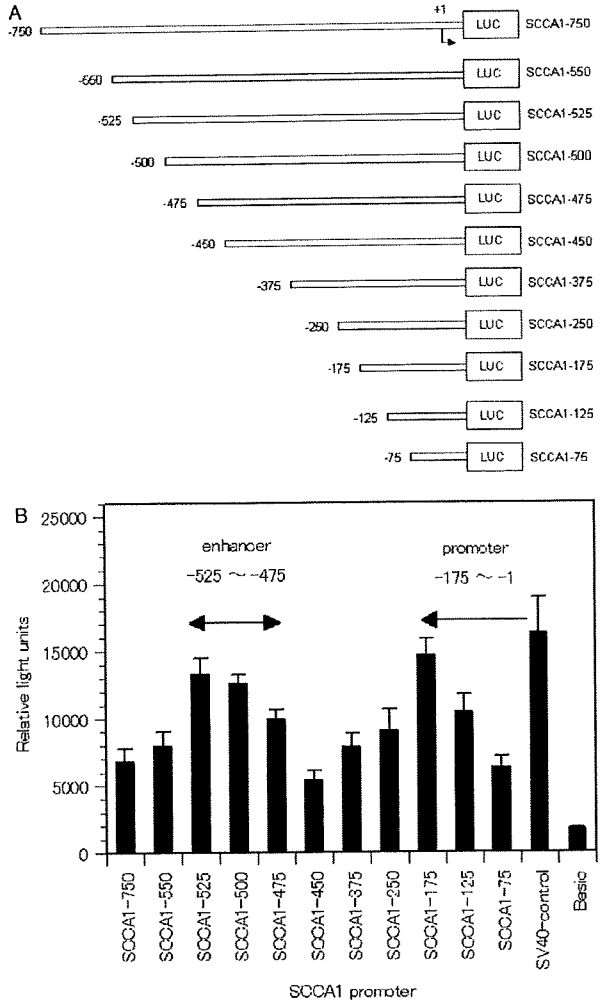

Figure 3. (A) A schematic representation of *SCCA1* reporter plasmids. 5′-truncated fragments of the promoter region upstream from the *SCCA1* gene were inserted into luciferase (LUC) reporter vector in sense orientation. Arrow indicates the transcription start site. Numbers indicate the number of bases upstream (−) or downstream (+) from the transcription start site. The name of each reporter construct was assigned according to the 5′-end nucleotide numbers of inserted promoter sequences, upstream of the transcription start site. (B) Transcriptional activity of *SCCA1* promoter in HT-III cell line, and identification of core promoter region. Bars indicate the SD

repeats of −525-bp to −475-bp) as shown in Figure 4A and transfected into HT-III cells, and cell lysates were tested in luciferase assays. Figure 4B demonstrates the transcriptional activities in HT-III cells. Intron 1 did not enhance SCCA1-175 promoter activity, consistent with a previous study [13]. However, the sense and antisense orientations of the −525-bp to −475-bp region significantly enhanced SCCA1-175 promoter activity, indicating that this region functioned as an enhancer for the SCCA1-175 promoter. Five tandem repeats of the −525-bp to −475-bp region increased SCCA1-175 promoter activity by up to four-fold, whereas ten or 20 tandem repeats of this enhancer region did not further increase SCCA1-175 promoter activity compared to five tandem repeats.

To compare the tissue specificity of the transcriptional activity of enhancer-promoter complex of *SCCA1* promoter, various numbers of tandem repeats of enhancer and SCCA1-175 promoters were transfected into HT-III squamous cell carcinoma cells and H1299 adenocarcinoma cells. The promoter activity of SCCA1-175 in HT-III cells was 20-fold greater than that in H1299 cells, and the promoter activity of five tandem repeats of the enhancer and SCCA1-175 in HT-III cells was 37-fold greater than that in H1299 cells (Figure 4C). Thus, five tandem repeats of enhancer and promoter complex exhibited significant tissue specificity in squamous cell carcinoma cells compared to adenocarcinoma cells.

To compare the tissue specificity of transcriptional activity of the enhancer-promoter complex of *SCCA1* promoter, SCCA1-175 with five tandem repeats of enhancer and SCCA1-175 promoter were transfected into squamous cell carcinoma cells, normal keratinocytes, normal non-keratinocyte cells and adenocarcinoma cells. The promoter activity of SCCA1-175 in squamous cell carcinoma cells was 2.4-fold greater than that in keratinocyte cells, 7.6-fold greater than that in normal non-keratinocyte cells and 13-fold greater than that in adenocarcinoma cells (Figure 4D). The promoter activity of SCCA1-175 in normal keratinocytes was three-fold greater than that in non-keratinocyte cells and five-fold greater than that in adenocarcinoma cells. The promoter activity of five tandem repeats of enhancer and SCCA1-175 in squamous cell carcinoma cells was five-fold greater than that in keratinocytes, 16-fold greater than that in non-keratinocyte cells and 30-fold greater than that in adenocarcinoma cells. The promoter activity of five tandem repeats of enhancer and SCCA1-175 in keratinocytes was three-fold greater than that in non-keratinocyte cells and six-fold greater than that in adenocarcinoma cells. The promoter activities of SCCA1-175 and SCCA1-175 with tandem repeats of enhancer did not differ significantly between normal non-keratinocyte cells and adenocarcinoma cells. Thus, five tandem repeats of enhancer significantly increased SCCA1-175 promoter activity in squamous cell carcinoma cells compared to normal keratinocytes, normal non-keratinocyte cells and adenocarcinoma cells.

Transcriptionally targeted AdE3-*SCCA1* has a potent antiproliferative effect in squamous cell carcinoma cells but not in normal non-keratinocyte cells or adenocarcinoma cells

To estimate the potential of *SCCA1* promoter for use in gene therapy for squamous cell carcinoma, *SCCA1* promoter-driven oncolytic adenovirus was constructed and transfected into each cell line. Figure 5A shows the construct of oncolytic adenovirus AdE3-*SCCA1* in which the 404–551-bp region of *E1A* promoter was substituted

by five tandem repeats of enhancer and SCCA1-175 promoter complex. Figure 5B shows the growth-inhibitory effects (IC_{50}) of oncolytic adenovirus AdE3-*SCCA1* in various types of cell lines. The IC_{50} of wild-type adenovirus AdE3 did not differ significantly among squamous cell carcinoma cells, normal keratinocytes, normal non-keratinocyte cells, nor adenocarcinoma cells. AdE3-*SCCA1* killed neither normal non-keratinocyte cells,

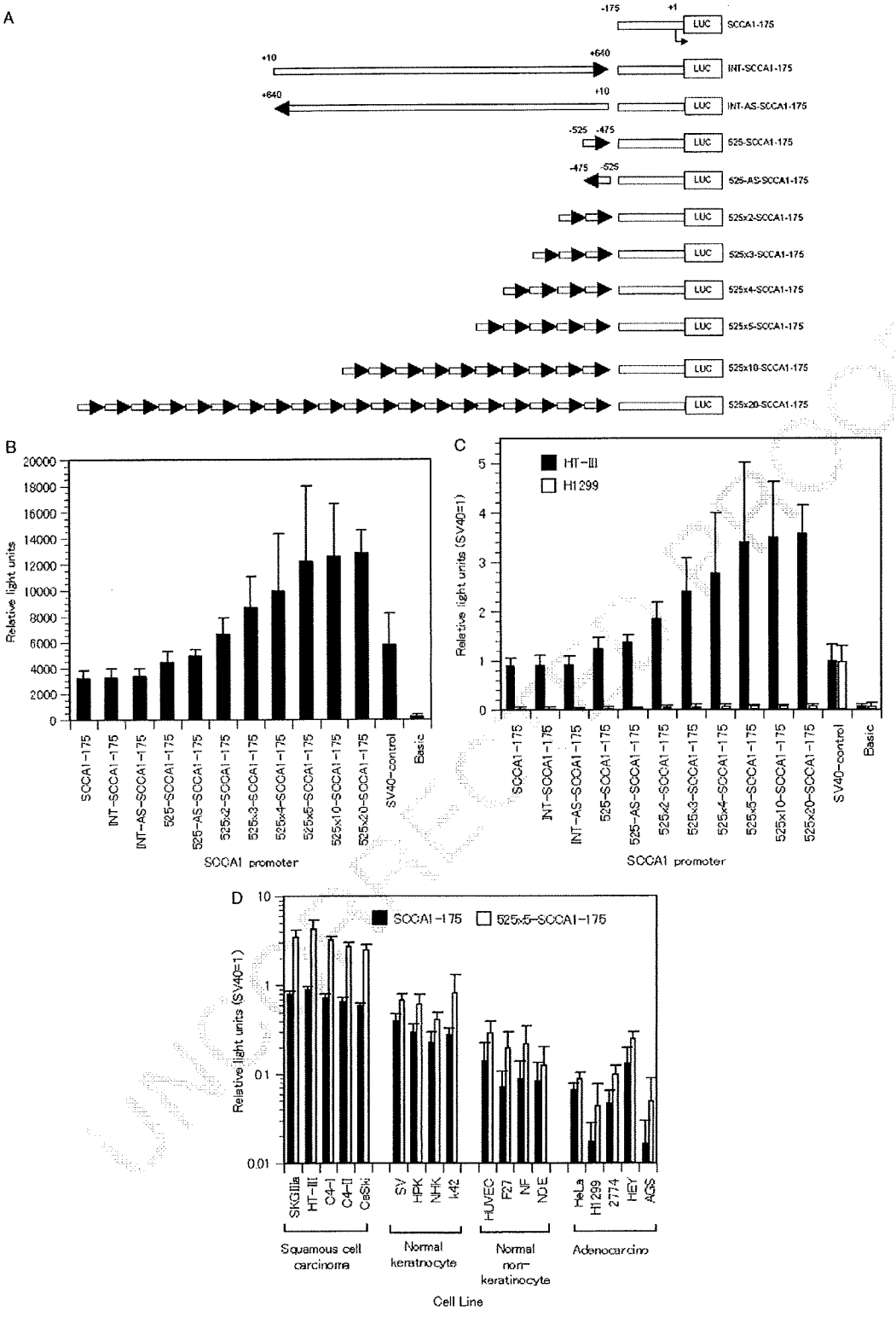

Figure 4.

DOI: 10.1002/jgm

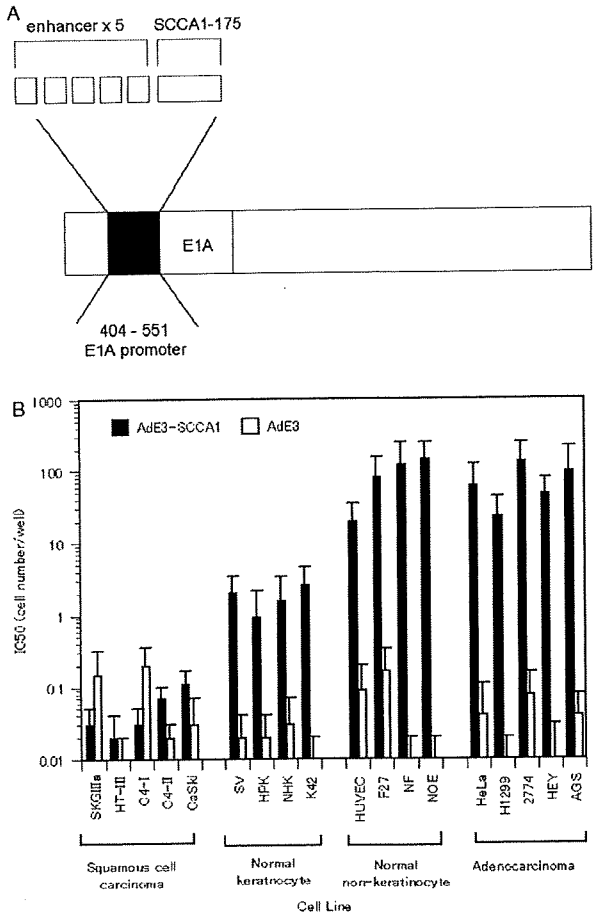

Figure 5. (A) A schematic representation of oncolytic adenovirus AdE3-*SCCA1*. SCCA1-175 with five tandem repeats from −525 to −475 bp was replaced with 404–551 bp of *E1A* promoter region. (B) The growth-inhibitory effects (IC_{50}) of oncolytic adenovirus AdE3-*SCCA1* and wild-type adenovirus AdE3 in cervical squamous cell carcinoma, normal keratinocyte, normal non-keratinocyte and adenocarcinoma cell lines. Bars indicate the SD

nor adenocarcinoma cells. AdE3-*SCCA1* significantly suppressed the growth of normal keratinocytes compared to normal non-keratinocyte cells and adenocarcinoma cells. Furthermore, this growth-inhibitory effect of AdE3-*SCCA1* was significantly enhanced in squamous cell carcinoma cells, and was one or two orders of magnitude higher than in normal keratinocytes.

Oncolytic adenovirus AdE3-*SCCA1* suppresses subcutaneous tumor growth of squamous cell carcinoma in nude and syngeneic mice

To evaluate the antitumor effects of AdE3-*SCCA1*, xenograftic subcutaneous tumors were established in the flanks of nude mice using cervical cancer HT-III and adenocarcinoma H1299 cells (Figure 6A). By 30 days, we observed a significant reduction in tumor size in the AdE3-*SCCA1*- and AdE3-treated groups compared to the medium alone- and Ad5CMV-*LacZ*-treated groups in the HT-III tumor models. AdE3-*SCCA1* and AdE3 significantly reduced tumor sizes by 95–98% compared to medium alone and Ad5CMV-*LacZ* ($p < 0.001$, unpaired *t*-test) (Figure 6B). By contrast, AdE3-*SCCA1* did not significantly reduce the sizes of H1299 tumors compared to Ad5CMV-*LacZ* (Figure 6C). However, AdE3 significantly reduced the size of H1299 tumors by 96% compared to Ad5CMV-*LacZ* ($p < 0.001$, unpaired *t*-test).

To evaluate the antitumor effects of AdE3-*SCCA1* after immunization, C3H mice were immunized with Ad5CMV-*LacZ* and subcutaneous tumors 5–8 mm in diameter were established in the left thigh of C3H mice using mouse squamous carcinoma SCC7 cells (Figure 7A). The survival of control mice was not significantly different from that of the mice treated with AdE3-*SCCA1* alone. We screened the 16 cell types of cells found to function as carrier cells for 293 and A549 cells [14]. Because A549 cells infected with oncolytic adenovirus were less damaged by freezing and thawing than 293 cells infected with oncolytic adenovirus, we used A549 cells as carrier cells. The A549 carrier cells all died within 2 weeks. The survival of mice treated with A549 carrier cells infected with AdE3-*SCCA1* was significantly longer than that of mice treated with medium control or AdE3-*SCCA1*. Furthermore, simultaneous infection with AxCA*mGM-CSF* augmented the antitumor effect of A549 carrier cells infected with AdE3-*SCCA1* ($p < 0.05$) (Figure 7B). Mice that exhibited complete tumor regression were resistant to subsequent inoculation of SCC7 cells.

Figure 4. (A) A schematic representation of *SCCA1* reporter plasmids with tandem repeats of enhancer region. The intron 1 region or proximal promoter region from −525-bp to −475-bp in sense or antisense orientation was inserted into upstream of the 175-bp region of *SCCA1* luciferase promoter plasmid. Tandem repeats of proximal promoter region from −525-bp to −475-bp were inserted into upstream of the 175-bp region of *SCCA1* luciferase promoter plasmid. (B) Luciferase activity of each reporter plasmid was examined in cervical squamous cell carcinoma HT-III. The plasmid (pGV-control) driven by SV40 enhancer/promoter was used as a positive control and pGV-Basic without enhancer/promoter as a negative control. Bars indicate the SD. (C) Luciferase activity of each reporter plasmid was examined in cervical squamous cell carcinoma HT-III and adenocarcinoma H1299 cells. The plasmid (pGV-control) driven by SV40 enhancer/promoter was used as a positive control and pGV-Basic without enhancer/promoter as a negative control. Luciferase activity in each plasmid was plotted as the ratio to the positive control plasmid (pGV-control). Bars indicate the SD. (D) Luciferase activities of reporter plasmids SCCA1-175 and SCCA1-175 inserted with five tandem repeats from −525 to −475 bp were examined in cervical squamous cell carcinoma, normal keratinocyte, normal non-keratinocyte and adenocarcinoma cells. The plasmid (pGV-control) driven by SV40 enhancer/promoter was used as a positive control and luciferase activity in each cell line was plotted as the ratio to the positive control plasmid. Bars indicate the SD

DOI: 10.1002/jgm

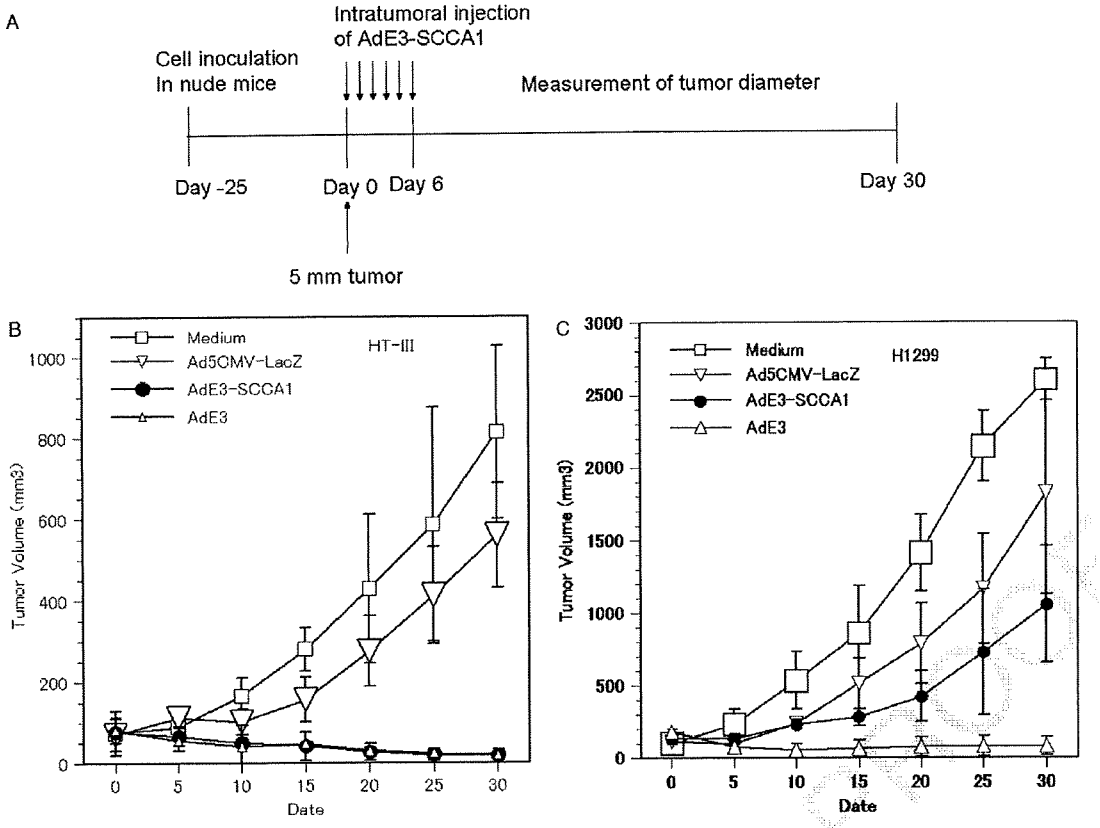

Figure 6. (A) A schematic representation of treatment schedule of oncolytic adenovirus AdE3-*SCCA1* in nude mice. (B) The antitumor effect of AdE3-*SCCA1* in subcutaneous cervical squamous cell carcinoma HT-III cell tumors in nude mice. (C) The antitumor effect of AdE3-*SCCA1* against subcutaneous adenocarcinoma H1299 cell tumors in nude mice

Discussion

In the present study, the highest *SCCA1* promoter activities were found in the 175-bp region just upstream of the *SCCA1* gene. It has been reported that a 0.5-kb fragment upstream of the *SCCA1* gene exhibited significant promoter activity [8]. This is consistent with the enhancer region and promoter activity identified in the present study. The negative element in the region 0.3- to 0.4-kb upstream of the *SCCA1* gene was reported previously [15], and corresponds to the negative 250- to 450-bp region in the present study. The positive 175-bp *SCCA1* promoter element had not been previously reported because the promoter activity of the 0- to 200-bp fragment of the *SCCA1* gene remained to be determined. The present study is thus the first to report promoter analysis of the proximal region of the *SCCA1* promoter and determine the maximal promoter activity of the 175-bp fragment of the *SCCA1* gene.

The present study also revealed an enhancer region 475-bp to 525-bp upstream of *SCCA1*. It has been reported that intron 1 in sense orientation alone increased 0.3-kb *SCCA1* promoter activity by two-fold, whereas that in antisense orientation did not increase it [15]. However, intron 1 in neither sense, nor antisense orientation increased *SCCA1* promoter activity in the present study, suggesting that intron 1 is not a major enhancer of *SCCA1*. Instead, we found that the 475-bp to 525-bp fragment increased SCCA1-175 promoter activity by 50% in sense and antisense orientations. The 475-bp to 525-bp fragment thus appears to be a major enhancer region of *SCCA1*. Double and triple enhancers further increased promoter activity compared to the single enhancer in the present study. Use of five tandem repeats of minimum enhancer element increased promoter activity the most, by four-fold, compared with one to four, ten or 20 tandem repeats of the enhancer element. Thus, five tandem repeats of minimum enhancer element significantly increased promoter activity and might enhance the amplification and the antitumor effects of replication-competent adenovirus.

SCCA protein, *SCCA1* mRNA, and *SCCA2* mRNA levels and SCCA1-175 promoter activity in squamous cell carcinoma cells were significantly higher than those in normal keratinocytes, which were in turn significantly higher than those in normal non-keratinocytes and adenocarcinoma cells. Although comparisons of *SCCA* gene expression and promoter activity among squamous cell carcinoma cells, normal keratinocytes and adenocarcinoma cells were reported previously [8,10], comparisons among squamous cell carcinoma cells, normal keratinocytes and normal non-keratinocyte cells had not previously

DOI: 10.1002/jgm

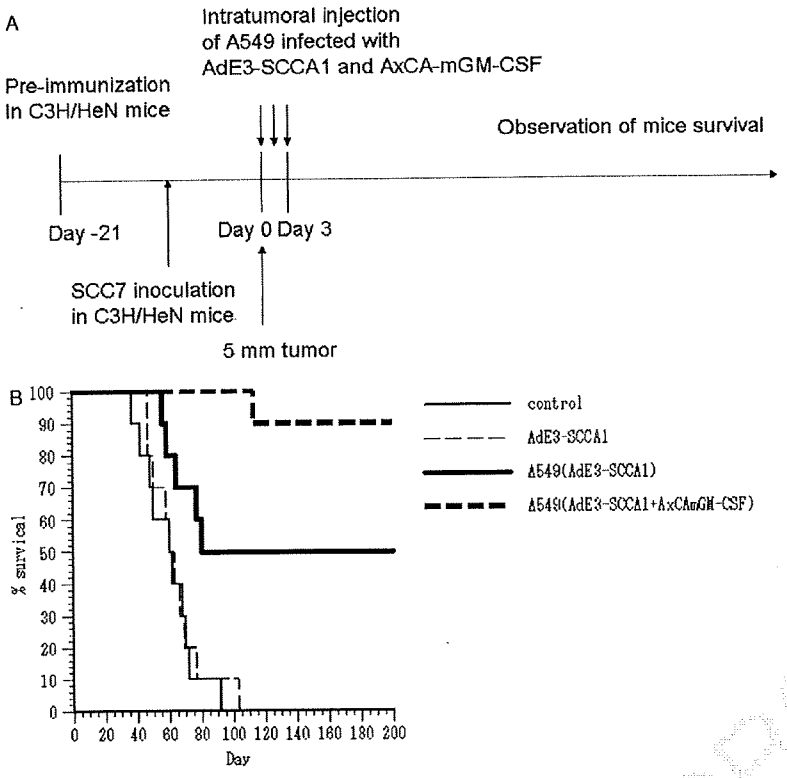

Figure 7. (A) A schematic representation of treatment schedule of carrier cells infected with oncolytic adenovirus AdE3-*SCCA1* and AxCA-*mGM-CSF* in syngeneic C3H/HeN mice. (B) The antitumor effects of AdE3-*SCCA1* against subcutaneous SCC7 tumors established in C3H mice after immunization. RPMI medium, AdE3-*SCCA1*, A549 carrier cells infected with AdE3-*SCCA1*, and A549 carrier cells infected with AdE3-*SCCA1* and AxCA*mGM-CSF* were injected into each tumor

been performed. SCCA1-175 and 525-5-SCCA1-175 promoter activities in normal keratinocytes were significantly higher than those in normal non-keratinocyte cells, and oncolytic adenovirus AdE3-*SCCA1* significantly suppressed the *in vitro* growth of normal keratinocyte cells compared to that of normal non-keratinocyte cells. These findings suggest that the *SCCA1* promoter might also be useful for gene therapy for skin diseases other than cancer.

The *SCCA1* to *SCCA2* mRNA ratio in squamous cell carcinoma cells was significantly lower than that in the other cells examined because the relative increase in *SCCA2* mRNA was significantly higher than that in *SCCA1* mRNA in squamous cell carcinoma cells compared to other cells. The adenovirus-mediated *SCCA2* promoter-driven proapoptotic gene thus induced selective tumor suppression of squamous cell carcinoma cells compared to adenocarcinoma cells [11], although this was not sufficient to induce complete tumor regression because *SCCA1* promoter activity is higher than *SCCA2* promoter activity in squamous cell carcinoma cells. We therefore used the *SCCA1* promoter for gene therapy for squamous cell carcinoma cells. Furthermore, although *SCCA1* promoter alone was not sufficient for overexpression of genes, five tandem repeats of enhancer increased *SCCA1* promoter activity by four-fold and increased the selectivity for squamous cell carcinoma by two-fold compared to that for the other cells examined.

The oncolytic adenovirus AdE3-*SCCA1* selectively killed squamous cell carcinoma cells *in vitro* and *in vivo*. Squamous cell carcinoma can occur in many different organs, including the skin, lips, mouth, oesophagus, urinary bladder, prostate, lungs, vagina and cervix, amongst others. Although oncolytic adenovirus vector driven by *SCCA2* promoter [11] has been reported, *SCCA1* promoter-driven oncolytic virotherapy has not. The present study is the first report of *SCCA1*-specific gene therapy. In clinical trials for squamous cell carcinoma, although adenovirus-*p53* for head and neck cancer [16], lung cancer [17], and esophageal cancer [18] and replicative oncolytic adenovirus for head and neck caner [19] have been reported, the results of such clinical trials were clinically insufficient because adenoviral infection was completely blocked by the production of anti-adenovirus antibody. This finding is identical to those for gene therapy with other viruses. It has been reported that oncolytic virus-infected carrier cells overcome the viral-induced humoral immune response, that the viral-induced cellular immune response kills virus-infected target cancer cells, and that granulocyte macrophage colony-stimulating factor augments the antitumor effect of carrier cells [14]. The present study also demonstrated that oncolytic adenovirus-infected A549 carrier cells induced elimination of tumor and that adenovirus-*GM-CSF* augmented the antitumor effect

of carrier cells, which induced complete regression of tumor in 90% of mice. Furthermore, a second challenge of syngeneic mouse squamous cell carcinoma was completely rejected by a specific antitumor response, also suggesting that the systemic tumor immune response induced by carrier cell treatment may cure not only carrier cell-injected local tumors, but also non-injected metastatic tumors. In conclusion, *SCCA1* promoter-driven oncolytic adenovirus-infected carrier cells may cure human squamous cell carcinoma of the head and neck, skin, oesophagus, lung, cervix, and other organs, and human clinical trials of these squamous cell carcinoma-specific carrier cells should be possible in the near future.

Acknowledgements

This study was supported by a grant from the Ministry of Education, Science, Sports and Culture, Japan, and by the Integrated Center for Science, Ehime University. We thank K. Oka for preparing culture medium and S. Hirose for comments and discussion. The authors have no conflicting financial interests to declare.

References

1. Takeshima N, Suminami Y, Takeda O, Abe H, Okuno N, Kato H. Expression of mRNA of SCC antigen in squamous cells. *Tumor Biol* 1992; **13**: 338–342.
2. Kato H, Torigoe H. Radioimmunoassay for tumor antigen of human cervical squamous cell carcinoma. *Cancer* 1977; **40**: 1621–1628.
3. Senekjian EK, Young JM, Weiser PA, Spencer CE, Magic SE, Herbst AL. An evaluation of squamous cell carcinoma antigen in patients with cervical squamous cell carcinoma. *Am J Obstet Gynecol* 1987; **157**: 433–439.
4. Bolli JA, Doering DL, Bosscher JR, *et al.* Squamous cell carcinoma antigen: clinical utility in squamous cell carcinoma of the uterine cervix. *Gynecol Oncol* 1994; **55**: 169–173.
5. Duk JM, de Bruijn HXA, Groenier KH, *et al.* Cancer of the uterine cervix: sensitivity and specificity of serum squamous cell carcinoma antigen determinations. *Gynecol Oncol* 1990; **39**: 186–194.
6. Takeshima N, Hirai Y, Katase K, Yano K, Yamauchi K, Hasumi K. The value of squamous cell carcinoma antigen as a predictor of nodal metastasis in cervical cancer. *Gynecol Oncol* 1998; **68**: 263–266.
7. Schneider SS, Schick C, Fish KE, *et al.* A serine proteinase inhibitor locus at 18q21.3 contains a tandem duplication of the human squamous cell carcinoma antigen gene. *Proc Natl Acad Sci USA* 1995; **92**: 3147–3151.
8. Hamada K, Shinomiya H, Asano Y, *et al.* Molecular cloning of human squamous cell carcinoma antigen 1 gene and characterization of its promoter. *Biochim Biophys Acta* 2001; **91522**: 1–8.
9. Sakaguchi Y, Kishi F, Murakami A, Suminami Y, Kato H. Structural analysis of human SCC antigen 2 promoter. *Biochim Biophys Acta* 1999; **1444**: 111–116.
10. Hamada K, Hanakawa Y, Hashimoto K, *et al.* Gene expression of human squamous cell carcinoma antigens 1 and 2 in human cell lines. *Oncol Rep* 2001; **8**: 347–54.
11. Hsu KF, Wu CL, Huang SC, *et al.* Conditionally replicating E1B-deleted adenovirus driven by the squamous cell carcinoma antigen 2 promoter for uterine cervical cancer therapy. *Cancer Gene Ther* 2008; **15**: 526–534.
12. Hamada K, Kohno S, Iwamoto M, *et al.* Identification of the human IAI.3B promoter element and its use in the construction of a replication-selective adenovirus for ovarian cancer therapy. *Cancer Res* 2003; **63**: 2506–2512.
13. Latham JPF, Searle PF, Mautner V, James ND. Prostate-specific antigen promoter/enhancer driven gene therapy for prostate cancer: construction and testing of a tissue-specific adenovirus vector. *Cancer Res* 2000; **60**: 334–341.
14. Hamada K, Desaki J, Nakagawa K, Shirakawa T, Gotoh A, Tagawa M. Carrier cell-mediated infection of a replication-competent adenovirus for cancer gene therapy. *Mol Ther* 2007; **15**: 1121–1128.
15. Suminami Y, Kishi F, Nawata S, *et al.* Promoter analyses of SCC antigen genes. *Biochim Biophys Acta* 2005; **1727**: 208–212.
16. Clayman GL, el-Naggar AK, Lippman SM, *et al.* Adenovirus-mediated p53 gene transfer in patients with advanced recurrent head and neck squamous cell carcinoma. *J Clin Oncol* 1998; **16**: 2231–2232.
17. Fujiwara T, Tanaka N, Kanazawa S, *et al.* Multicenter phase I study of repeated intratumoral delivery of adenoviral p53 in patients with advanced non-small-cell lung cancer. *J Clin Oncol* 2006; **24**: 1689–1699.
18. Shimada H, Matsubara H, Shiratori T, *et al.* Phase I/II adenoviral p53 gene therapy for chemoradiation resistant advanced esophageal squamous cell carcinoma. *Cancer Sci* 2006; **97**: 554–561.
19. Nemunaitis J, Khuri F, Ganly I, *et al.* Phase II trial of intratumoral administration of ONYX-015, a replication-selective adenovirus, in patients with refractory head and neck cancer. *J Clin Oncol* 2001; **19**: 289–298.

QUERIES TO BE ANSWERED BY AUTHOR

IMPORTANT NOTE: Please mark your corrections and answers to these queries directly onto the proof at the relevant place. Do NOT mark your corrections on this query sheet.

Queries from the Copyeditor:

AQ1 '3000 r.p.m.'. Please provide 'g' value

AQ2 'LIFETEST procedure'. Please provide the details of any software package used (i.e. manufacturer and manufacturer's location or a URL from where it can be obtained)

British Journal of Cancer (2010) 102, 206–212

www.bjcancer.com

Gene set enrichment analysis provides insight into novel signalling pathways in breast cancer stem cells

M Murohashi[1,6], K Hinohara[1,6], M Kuroda[2], T Isagawa[3], S Tsuji[3], S Kobayashi[4], K Umezawa[5], A Tojo[4], H Aburatani[3] and N Gotoh[*,1]

[1]Division of Systems Biomedical Technology, Institute of Medical Science, University of Tokyo, Tokyo, Japan; [2]Department of Pathology, Tokyo Medical University, Tokyo, Japan; [3]Genome Science Division, Research Center of Advanced Science and Technology, University of Tokyo, Tokyo, Japan; [4]Division of Molecular Therapy, Institute of Medical Science, University of Tokyo, Tokyo, Japan; [5]Department of Applied Chemistry, Faculty of Science and Technology, Keio University, Yokohama, Japan

BACKGROUND: Tumour-initiating cells (TICs) or cancer stem cells can exist as a small population in malignant tissues. The signalling pathways activated in TICs that contribute to tumourigenesis are not fully understood.

METHODS: Several breast cancer cell lines were sorted with CD24 and CD44, known markers for enrichment of breast cancer TICs. Tumourigenesis was analysed using sorted cells and total RNA was subjected to gene expression profiling and gene set enrichment analysis (GSEA).

RESULTS: We showed that several breast cancer cell lines have a small population of $CD24^{-/low}/CD44^{+}$ cells in which TICs may be enriched, and confirmed the properties of TICs in a xenograft model. GSEA revealed that $CD24^{-/low}/CD44^{+}$ cell populations are enriched for genes involved in transforming growth factor-β, tumour necrosis factor, and interferon response pathways. Moreover, we found the presence of nuclear factor-κB (NF-κB) activity in $CD24^{-/low}/CD44^{+}$ cells, which was previously unrecognised. In addition, NF-κB inhibitor dehydroxymethylepoxyquinomicin (DHMEQ) prevented tumourigenesis of $CD24^{-/low}/CD44^{+}$ cells *in vivo*.

CONCLUSION: Our findings suggest that signalling pathways identified using GSEA help to identify molecular targets and biomarkers for TIC-like cells.

British Journal of Cancer (2010) **102,** 206–212. doi:10.1038/sj.bjc.6605468 www.bjcancer.com
Published online 8 December 2009

Keywords: tumour-initiating cells; NF-κB; CD24; CD44; gene expression profiling; DHMEQ

Accumulating evidence suggests that tumour-initiating cells (TICs) or cancer stem cells—which make up only a small proportion of heterogeneous tumour cells—possess a greater ability to maintain tumour formation than other tumour cell types. It has been proposed that TICs have characteristics in common with normal stem cells from tumour-prone tissue (Ailles and Weissman, 2007). For instance, TICs can self-renew and simultaneously produce differentiated daughter cells that proliferate strongly until they reach their final differentiated state. Apparent differences also exist between TICs and normal stem cells. The latter are maintained under tight homoeostatic regulation and are passively protected in the surrounding microenvironment or stem cell niche in adult tissues. However, the former may actively contribute to tumour formation. Although the concept of TICs greatly influences cancer biology and evokes a reconsideration of cancer treatment, the molecular mechanisms involved in the contribution of TICs to tumourigenesis remain obscure.

In human breast cancers, a population characterised by the expression of cell-surface markers, $CD24^{-/low}/CD44^{high}$, was reported to be highly enriched in TICs, compared with populations of $CD24^{high}/CD44^{high}$ cells (Al-Hajj *et al*, 2003; Mani *et al*, 2008). Two gene-expression profiling studies, comparing $CD24^{-/low}/CD44^{+}$ cell populations with other populations in primary breast cancer cells or in normal tissue, presented the $CD24^{-/low}/CD44^{+}$ cell population-derived different signatures that seemed to predict poorer prognosis (Liu *et al*, 2007; Shipitsin *et al*, 2007). One study showed that transforming growth factor (TGF)-β pathways seem to be activated in these cells (Shipitsin *et al*, 2007). It was subsequently reported that TGF-β induced the epithelial–mesenchymal transition (EMT) in mammary glands and stem-like cells in both normal mammary epithelial cells and breast cancer cells (Mani *et al*, 2008). Because TGF-β signalling can have positive or negative effects on tumourigenesis, additional signalling may still be needed to stimulate tumourigenesis.

Nuclear factor-κB (NF-κB) is a transcription factor complex and is typically a heterodimer of p50, p52, p65 (RelA), RelB, and c-Rel. It is usually inactive and bound to IκB, an inhibitory protein, in the cytoplasm. Upon stimulation with signals such as tumour

*Correspondence: Dr N Gotoh, Division of Systems Biomedical Technology, Institute of Medical Science, University of Tokyo, Tokyo, Japan; E-mail: ngotoh@ims.u-tokyo.ac.jp
[6]These authors contributed equally to this work.
Received 10 August 2009; revised 26 October 2009; accepted 9 November 2009; published online 8 December 2009